

Numerical simulations of an evaporating bio-oil droplet

J. D. Brett¹, A. Ooi¹ and J. Soria²

¹Department of Mechanical and Manufacturing Engineering
The University of Melbourne, Victoria, 3010 AUSTRALIA

²Laboratory for Turbulence Research in Aerospace and Combustion (LTRAC)
Department of Mechanical Engineering
Monash University, Victoria, 3800 AUSTRALIA

Abstract

Bio-oil is a promising alternative fuel which contains a wide range of chemical components, including high molecular mass, organic compounds and a significant amount of water. This chemical structure can lead to a slow evaporation rate with the low boiling point compounds like water evaporating away from the surface while significant proportions still remain in the droplet core due to the relatively slow rate of liquid diffusion. As the droplet temperature increases, this water trapped in the core can reach a sufficiently high temperature to cause it to vapourise resulting in the droplet exploding. This study presents a numerical model of a stationary spherically symmetric evaporating bio-oil droplet in a hot ambient atmosphere. A diffusion limited model is used to investigate the effect of the large number components, including high boiling point chemicals, on the droplet evaporation rate. The numerical model simulates transient behaviour in the liquid and vapour phases by solving diffusion and heat transport equations in both phases using temperature dependent fluid properties.

Introduction

An excellent in depth review of the field of droplet and spray modelling can be found in Sirignano's book [6]. Evaporation models can be divided into two categories, hydrodynamic and kinetic. Hydrodynamic models assume that the fuel vapour is saturated at the droplet surface, while in kinetic models a fraction of vapour molecules striking the liquid surface are reabsorbed into the liquid. A comparison of the hydrodynamic and kinetic models for diesel fuel was conducted by Kryukov *et al* [3], showing that the models produce slightly different results. However the kinetic model requires an accurately determined evaporation constant, β_m , which can be difficult to obtain. For this reason the model used in this paper follows the hydrodynamic approach. The first model of an evaporating droplet, the d^2 law, is a hydrostatic model, and can be expressed in the form published by Spalding [7] in 1953,

$$\left(\frac{d}{d_0}\right)^2 = 1 - \beta t, \quad (1)$$

where d is the droplet diameter at time t , d_0 is the diameter at $t = 0$ and β is a constant dependent upon the initial droplet size, temperature, liquid and gas properties. The d^2 law is based upon the assumption of a quasi-steady evaporating droplet, where the droplet temperature is in equilibrium with its surrounding and is constant with respect to both space and time.

The d^2 law is often used in simple evaporation models and it is not appropriate for systems where transient effects are significant, especially those where the droplet contains a diverse mix of components.

Bio-oil is oil created by the pyrolysis of biomass such as wood. If implemented in a continuously regrown cycle, the resultant

oil can be used as a CO₂ neutral source of fuel, with the amount of CO₂ being released by the combustion of the oil being absorbed by the regrowing of the biomass stock. When considered together with its ability to be created anywhere capable of growing vegetation this leads to a fuel of significant value. However bio-oil consists of a large number of chemical compounds, including a significant water content (typically between 15% and 30%), and heavy phenolic compounds. The presence of these complicates its use as a fuel. When modelling bio-oil the oil is typically represented by a series of groups to chemical groups. These groups can either be represented as continuous distributions (see Hallett and Clark [2]) or as a series of discrete components.

The heating and evaporation of fuel droplets is predominantly studied for use in engines where sprays of fuel droplets need to be vaporized and combusted. Incomplete evaporation can have a detrimental effect on power and emissions and is of particular concern in bio-oil applications where impurities in the fuel may result in the formation of char and lead to deposits on chamber walls, as discussed by Shaddix and Hardesty [5].

Hallett and Clark developed a numerical model for a stationary spherically symmetric bio-oil droplet, in which they represented the bio-oil composition with 4 continuous distributions, representing the acid, aldehyde/ketone, water and lignin fractions. They treated the liquid phase as well mixed, so that its composition and temperature was uniform, and included the breakdown of lignin to char and gas.

In this paper we investigate the heating and evaporation of stationary spherically symmetric bio-oil droplets using a numerical model with the bio-oil represented as discrete components. The discrete component approach was chosen over continuous gradients to allow for the inclusion of chemical reactions in the numerical model at a later date. The liquid phase has been modelled to allow for the development of concentration and temperature gradients.

Numerical model

This model considers a spherically symmetric droplet of radius R evaporating in a hot gas environment. Three regions are considered. The first region is inside the droplet ($r < R$), where the temperature profile is governed by thermal conduction. For a sphere with internal conduction, the heat balance equation can be expressed as,

$$\rho_l \hat{C}_l \frac{\partial T_l}{\partial t} = \frac{1}{r^2} \frac{\partial}{\partial r} \left(r^2 \lambda_l \frac{\partial T_l}{\partial r} \right), \quad (2)$$

where ρ_l is the density, \hat{C}_l is the constant pressure specific heat, λ_l is the thermal conductivity and T_l is the temperature of the liquid.

The temperature at the outer surface, T_s , of the droplet must

match the vapour temperature, and to ensure spherical symmetry and continuity, the center must have a zero temperature gradient. These boundary conditions can be written as,

$$T_{l,s} = T_s = T_{g,s} \quad (3)$$

at $r = R$ and

$$\frac{\partial T_l}{\partial r} = 0, \quad (4)$$

at $r = 0$, where the subscript l denotes liquid phase and g denotes the gas/vapour phase.

In the region surrounding the droplet ($r > R$) the temperature profile is governed by both thermal conduction and convection. Due to the assumption of spherical symmetry the only velocity is the radial velocity caused by the expansion of the fluid as it evaporates.

Applying the continuity equation to the gas phase leads to

$$r^2 \frac{\partial \rho_a}{\partial t} + \frac{\partial \rho_g u r^2}{\partial r} = 0, \quad (5)$$

where ρ_a is the density of the gas phase, and u is the radial velocity. The boundary conditions for vapour temperature are a constant far field temperature at the outer limit of the computational domain and Eq. (3) at the droplet surface.

With the assumption of constant pressure, the vapour velocity at the surface can be calculated as

$$u = \frac{\rho_l \dot{R} \rho_{as}}{\rho_g \rho_a}, \quad (6)$$

where ρ_{as} is the density of the gas phase at the droplet surface and ρ_g is the density of the fuel vapour at the surface conditions.

The surface temperature of the droplet is evaluated by energy conservation. The surface of the gas and liquid phases is assumed to be at equal temperatures, denoted T_s . The energy conservation equation balances the heat flow from the gas with the heat flowing into the droplet interior and the energy used to vaporise the liquid and is given by

$$\lambda_g R^2 \frac{dT_g}{dr} \Big|_s = \lambda_l R^2 \frac{dT_l}{dr} \Big|_s + \dot{R} L \rho_l. \quad (7)$$

This can be discretised spatially using a finite difference scheme and rearranged to solve for T_s .

The rate of evaporation, expressed as a change in radius can be calculated from mass balance to be

$$\dot{R} = \frac{\rho_g}{\rho_l (1 - Y_{fs})} \left(\frac{\partial Y_f}{\partial r} \right)_s \quad (8)$$

where Y_f is the molar concentration of the fuel vapour in the surrounding atmosphere. This concentration is calculated from diffusion using the following equation

$$\frac{\partial \rho_g r^2 Y_f}{\partial t} + \frac{\partial \rho_g u r^2 Y_f}{\partial r} - \frac{\partial \rho D r^2 \frac{\partial Y_f}{\partial r}}{\partial r} = 0, \quad (9)$$

D is the coefficient of diffusivity for the vapour in air. Y_f is assumed to asymptote to a constant far field ambient condition

(0 in this study). The concentration at the surface is calculated using the Clausius Clapeyron equation as,

$$Y_f = \frac{P_v}{P} = \frac{P_{ref}}{P} e^{(LM/\bar{R})(\frac{1}{T_{ref}} - \frac{1}{T_s})}, \quad (10)$$

where L is the latent heat of vapourisation, M is the Molar mass, \bar{R} is the ideal gas constant P is the ambient pressure and P_{ref} and T_{ref} are the vapour pressure and temperature of the gas at a known reference state.

The internal liquid diffusion can be calculated from conservation of matter, using the Maxwell-Stefan equations for molecular flux,

$$(J) = -c_t [B]^{-1} [\Gamma] (\nabla Y). \quad (11)$$

where

$$(J) = \begin{pmatrix} J_1 \\ J_2 \\ \vdots \\ J_{n-1} \end{pmatrix} \quad (\nabla Y) = \begin{pmatrix} \nabla Y_1 \\ \nabla Y_2 \\ \vdots \\ \nabla Y_{n-1} \end{pmatrix} \quad (12)$$

and the diffusivity matrix, $[B]$, and thermodynamic factor, $[\Gamma]$, are square matrices of size $n-1$. ∇Y_i is the spacial derivative of Y_i , the Molar concentration of fuel species i , in the direction of the diffusion calculation, and c_t is the Molar density of the fluid (Mole per volume). The flux of the last species, J_n , is calculated by balancing the system as follows,

$$\sum_{i=1}^n J_i = 0. \quad (13)$$

The thermodynamic factor, $[\Gamma]$, incorporates molecular interactions into the diffusion model. For this study these interactions were assumed to be small, allowing $[\Gamma]$ to be approximated by the identity matrix. The elements of $[B]$ are given by,

$$B_{ii} = \frac{x_i}{D_{in}} + \sum_{\substack{k=1 \\ i \neq k}}^n \frac{x_k}{D_{ik}}, \quad (14)$$

and

$$B_{ij} = -x_i \left(\frac{1}{D_{ij}} - \frac{1}{D_{in}} \right) \quad (15)$$

where $i \neq j$.

The values of the Maxwell-Stefan coefficients of diffusion, D_{ij} , were found using the Vignes method,

$$D_{ij} = (D_{ij}^o)^{(x_j)} (D_{ji}^o)^{(x_i)}. \quad (16)$$

The infinite dilution diffusion coefficient, D_{ij}^o , is the diffusion coefficient for an infinitely weak solution of species i in species j . This diffusion coefficient can be estimated using an empirical formulation. We selected the the Wilke and Chang formulation (see Taylor and Krishna[8] for more details).

The equations detailed in this section were solved numerically in a C++ program, using finite difference methods and Runge-Kutta time stepping. All fluid properties were modelled as functions of temperature using experimental data (taken from Vargaftik [9]) where available. When experimental data as a

function of temperature was not available empirical estimations (sourced from Poling et al [4]) were used.

Results

Single Fuel Cases

The behaviour of single fuel droplets was modelled to provide a base case against which more complex models could be compared. n-Hexane droplets were chosen for this model as experimentally determined properties could be easily found. The ambient atmosphere was modelled at a temperature of 325K and a pressure of 100kPa, with the initial droplet temperature set at 300K. Droplets with initial radii of 5, 10 and 15 μm were simulated.

The radius as a function of time is shown in figure 1. All three droplets show the same expected trend, with a period of heating due to the initial liquid-gas temperature difference. This is followed by a curve that approximately follows the d^2 law behaviour of radius squared decreasing linearly with time.

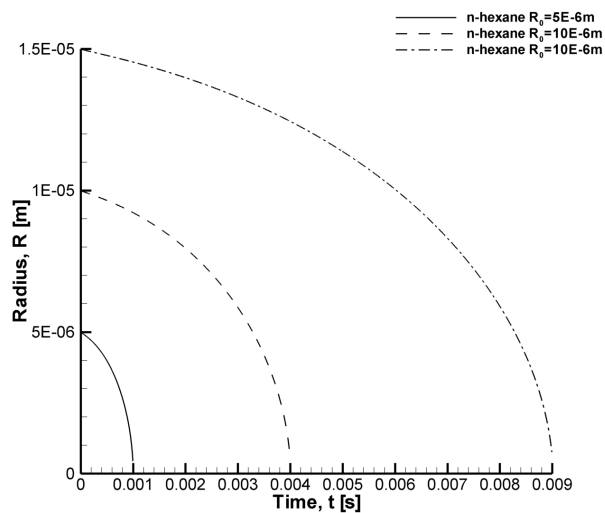


Figure 1: Radius versus time for single fuel cases

In the literature [6] it has been shown that the total evaporation time is proportional to the initial radius squared, R_0^2 . This was confirmed using the numerical model and the results are shown in figure 2. In this figure the time scale has been non-dimensionalised using the thermal diffusivity of the fuel, α_f , evaluated at a temperature of 300K. The radius has been non-dimensionalised using the initial radius and then squared. The results show excellent agreement with the three curves overlapping almost exactly, the non-dimensionalised radius squared values agree to five significant figures for most of the evaporation process and always agree to within three significant figures. They also show the linear decay of radius squared predicted by the d^2 law later in the droplet lifetime when the heating effect has reduced.

Bio-oil Cases

To create a model of bio-oil similar to that used by Hallett and Clark [2], 12 chemical components were chosen. The volume fractions were selected to approximate the continuous distributions specified in their paper. These chemicals are detailed in table 1.

The evolution of a droplet with time was simulated at two differ-

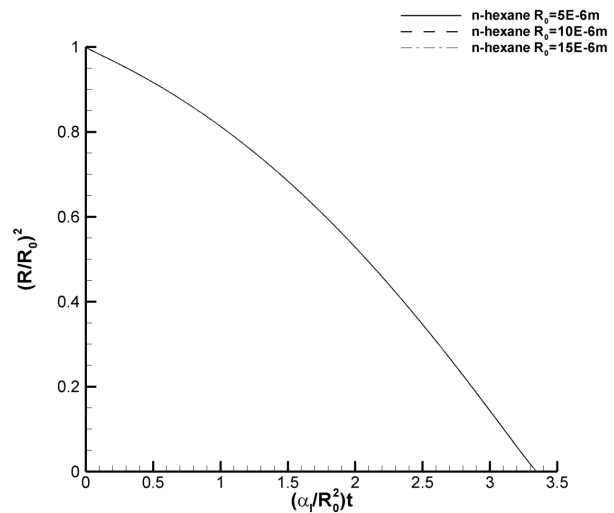


Figure 2: Non-dimensionalised radius squared versus non-dimensionalised time for single fuel cases.

ent temperatures (573K and 773K) to produce the results shown in figures 3 and 4. As the droplet was not assumed to remain evenly mixed while evaporating (i.e. for $t > 0$) concentration gradients for the low boiling point compounds evaporate at the droplet surface at a faster rate than the liquid diffusive mixing rate. This leads to the droplet surface becoming predominantly high-boiling point, non-evaporating compounds. At this point chemical reactions and oxidation become important, which can lead to the formation of solid cenospheres like those reported by García-Pérez et al [1]. For this reason results from our simulations are only presented up to the approximate point where all the lighter components have zero surface concentrations (after approximately 20 and 10 seconds respectively for the cases presented here).

Comparing the volume fraction graph (figures 3 and 4) to figures 5 and 6, which shows Hallett and Clark's simulated results it can be seen that our curve is less smooth. This is due to the discrete nature of our chemical representation, and the decrease of evaporation rate when concentrations at the surface reach zero. Figures 5 and 6 shows the evaporation stopping with approximately 45% of the initial mass remaining after 20 seconds for the low temperature case and 10 seconds for the high temperature, by contrast, due to the presence of lighter components in the droplet core and differences in droplet composition, our numerical model still has approximately 50% and 60%, respectively, of its initial volume, mostly consisting of the more dense components. This demonstrated that at higher temperatures, where the droplet evaporates faster, the importance of modelling liquid phase diffusion is higher.

The amounts of the individual components are shown in figures 7 and 8. Typically the evaporation rate is limited by the diffusion of vapour from the droplet surface into the far field. Distinct changes in volume fraction gradient are visible when concentrations at the surface reach zero, at which point the evaporation rate is limited by slower, liquid diffusion.

This sudden reduction in evaporation demonstrates the effect of heavy, non-volatile components on the usefulness of the fuel. Even a small initial fuel concentration can saturate the surface, leading to reduced evaporation rates, which in turn can lead to less than optimum combustion in turbines and internal combustion engines.

Table 1: Chemical compounds modelled to create a discrete representation of Hallett and Clark's [2] continuous bio-oil distribution

compound	chemical composition	molecular weight [g/mol]	initial volume fraction]
water	H ₂ O	18.02	0.267
acetaldehyde	C ₂ H ₄ O	44.05	0.144
propanal	C ₃ H ₆ O	58.08	0.109
butanal	C ₄ H ₈ O	72.11	0.021
pentanal	C ₅ H ₁₀ O	86.13	0.054
phenol	C ₆ H ₆ O	94.11	0.108
guaiacol	C ₇ H ₇ O ₂	124.14	0.042
coniferyl alcohol	C ₁₀ H ₁₂ O ₃	180.20	0.190
acetic acid	C ₂ H ₄ O ₂	60.05	0.037
propanoic acid	C ₃ H ₆ O ₂	74.08	0.017
butanoic acid	C ₄ H ₈ O ₂	88.11	0.008
pentanoic acid	C ₅ H ₁₀ O ₂	102.13	0.003

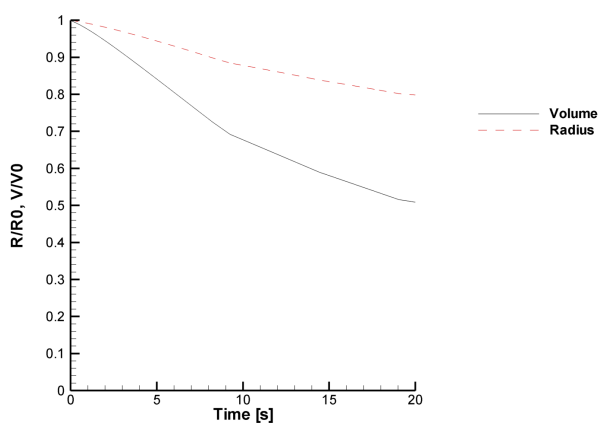


Figure 3: Droplet radius and volume as fractions of initial values for a 1.7mm bio-oil droplet evaporating at 573K

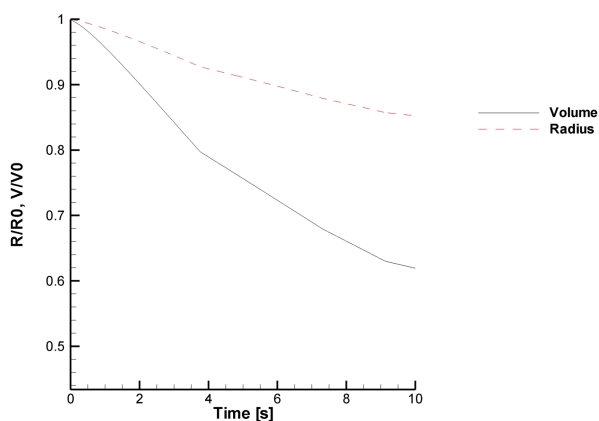


Figure 4: Droplet radius and volume as fractions of initial values for a 1.6mm bio-oil droplet evaporating at 773K

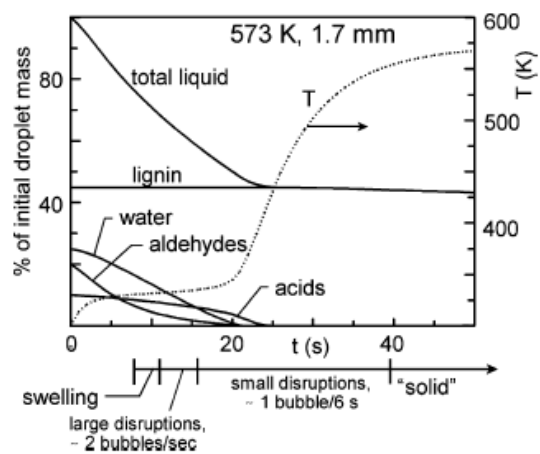


Figure 5: Droplet composition (expressed as fractions of initial mass) and temperature as a function of time for a 1.7mm bio-oil droplet evaporating at 573K, as predicted by Hallett and Clark. Observed droplet behaviour plotted below time scale. Initial droplet temperature 300K. Reproduced from [2]

The low boiling point chemicals inside the droplet can also reach their boiling point before fully evaporating. This leads to the formation of bubbles. Depending on the droplet size, composition and temperature, these bubbles will either force their way to the surface or cause micro-explosions, breaking the droplet up.

Conclusions

The limited rate of liquid diffusion was shown to have a significant effect on the evaporation of a stationary bio-oil droplet, especially at higher temperatures of evaporation. The presence of high boiling point chemicals significantly decreases the evaporation rate later in the droplet lifetime. This means that the benefits for processing bio-oil to remove or reduce these components would extend beyond the direct increase in the calorific value of the fuel. Reduced concentrations of heavy components would also reduce micro-explosions and bubbling effects. Long term goals for this model include simulating experimental studies for further model validation and the use in modelling bio-oils sprays in engines.

Acknowledgements

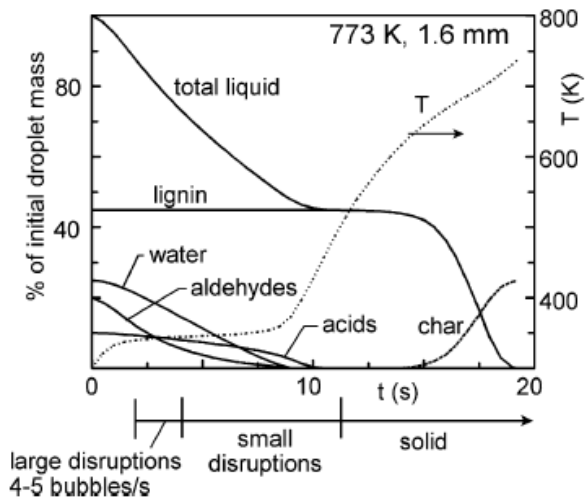


Figure 6: Droplet composition (expressed as fractions of initial mass) and temperature as a function of time for a 1.6mm bio-oil droplet evaporating at 773K, as predicted by Hallett and Clark. Observed droplet behaviour plotted below time scale. Initial droplet temperature 300K. Reproduced from [2]

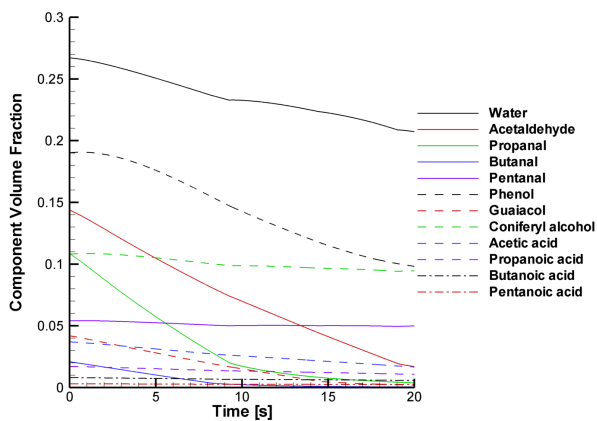


Figure 7: Component volume fractions (of initial droplet volume) for a 1.7mm bio-oil droplet evaporating at 573K

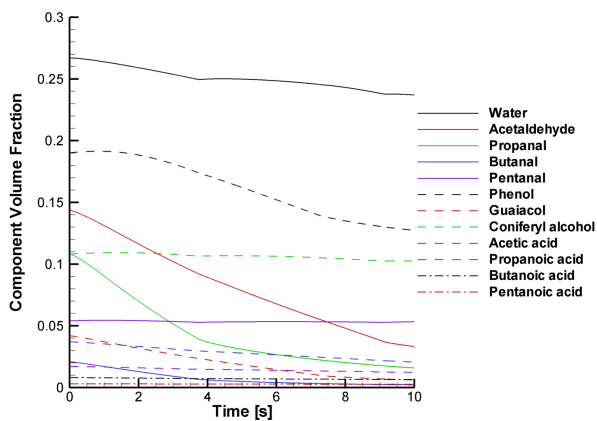


Figure 8: Component volume fractions (of initial droplet volume) for a 1.6mm bio-oil droplet evaporating at 773K

The authors would like to acknowledge the support of the ARC for this research through grant DP0556098.

References

- [1] M. García-Pérez and P. Lappa and P. Hughes and L. Dell and A. Chaala and D. Kretschmer and C. Roy, Evaporation and Combustion Characteristics of Biomass Pyrolysis Oils, *IFRF Combustion Journal*, 2006.
- [2] W. L. H. Hallett and N. A. Clark, A model for the evaporation of biomass pyrolysis oil droplets, *Fuel*, **85**, 2006, 532–544.
- [3] A. P. Kryukov and V. Y. Levashov and S. S. Sazhin, Evaporation of diesel fuel droplets: kinetic versus hydrodynamic models, *Int. J. Heat Mass Transfer*, **47**, 2004, 2541–2549.
- [4] B. E. Poling and J. M. Prausnitz and J. P. O'Connell, *The Properties of Gases and Liquids*. Fifth Edition, McGraw-Hill, 2001.
- [5] C. R. Shaddix and D. R. Hardesty, *Combustion Properties of Biomass Flash Pyrolysis Oils: Final Project Report*, Sandia National Laboratories, 1999.
- [6] W. A. Sirignano, *Fluid Dynamics and Transport of Droplets and Sprays*, Cambridge University Press, 1999.
- [7] D. B. Spalding, The combustion of liquid fuels, *Proc. 4th Symposium (Int.) on Combustion*, 1953, 847–864.
- [8] R. Taylor and R. Krishna, *Multicomponent Mass Transfer*, John Wiley & Sons, 1993.
- [9] N. B. Vargaftik, *Handbook of physical properties of liquids and gases: Pure substances and mixtures*. Second Edition, Hemisphere Publishing, 1975.